

## Tetrazolate–azido–copper(II) coordination polymers: tuned synthesis, structure, and magnetic properties†

Cite this:  
*CrystEngComm*,  
 2015, 17,  
 4136

Ya-Bo Xie,<sup>a</sup> Lei Gan,<sup>a</sup> E. Carolina Sañudo,<sup>b</sup> Haiyang Zheng,<sup>a</sup> Jiongpeng Zhao,<sup>a</sup> Minjian Zhao,<sup>a</sup> Bin Wang<sup>a</sup> and Jian-Rong Li<sup>\*a</sup>

As the first example of using a parent tetrazole and an azide together in preparing magnetic complexes, two novel tetrazolate–azido-bridged Cu(II) coordination polymers,  $[Cu(tz)(N_3)]_n$  (1) and  $[Cu(tz)(N_3)(NH_3)_2]_n$  (2) (tz = tetrazolate), have been synthesized through the reaction of Htz, CuCl<sub>2</sub>, and NaN<sub>3</sub> under hydrothermal conditions and in ammonia solution at room temperature, respectively. Single crystal X-ray structure analysis reveals that the two complexes possess distinct three-dimensional (3D) framework structures and can be topologically described as a 3-connected *srs* (SrSi<sub>2</sub>)-type net and a 4-connected *cds* (CdSO<sub>4</sub>)-type net, respectively. Both tetrazolate and azide groups also have different linkage modes in the two complexes. 1 contains end-on (EO) type azide bridges and 3-connected tetrazolate, while 2 possess end-to-end (EE) azide linkers and 2-coordinated tetrazolate. Magnetic measurements indicate that anti-ferromagnetic interactions dominate between Cu(II) ions in the two complexes with the corresponding magnetic coupling constant being  $J = -41.0 \text{ cm}^{-1}$  in 1 and  $J = -8.62 \text{ cm}^{-1}$  in 2.

Received 14th March 2015,  
 Accepted 21st April 2015

DOI: 10.1039/c5ce00531k

www.rsc.org/crystengcomm

## Introduction

Investigation into the structural and magnetic properties of transition metal complexes has become a fascinating subject in the field of coordination chemistry.<sup>1</sup> A common synthetic approach to molecular magnetic materials is to integrate paramagnetic centers with suitable bridging ligands to fabricate complexes that can give rise to magnetic exchange coupling. Besides the metal centers, the nature and linking modes of the bridging ligand also play crucial roles in tuning the bulk magnetic properties of resulting complexes. Therefore, the search and exploration for appropriate bridging ligands is a long-standing task in this field.

As a pseudohalide anion, the linear azide ion, having a rich variety of coordination modes (Scheme 1) and being a good mediator for transmitting magnetic coupling between paramagnetic metal centers because of its short length, has been widely utilized as a bridging ligand in the construction of magnetic materials with interesting structural and

magnetic features.<sup>1a,2</sup> When acting as a bridging ligand, there are two typical coordination modes of the azide ion: end-to-

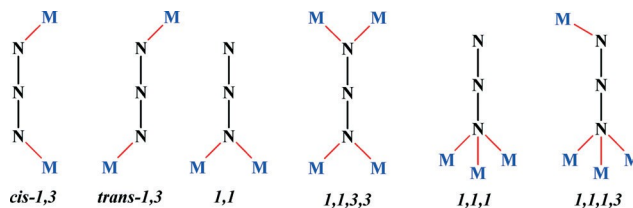
end (EE or 1,3) and end-on (EO or 1,1) modes. Normally, the end-to-end (EE) coordination mode gives antiferromagnetic coupling while the end-on (EO) mode transfers ferromagnetic coupling.<sup>3</sup> Despite the richness of metal–azide structural chemistry, only a few three-dimensional (3D) coordination networks<sup>1a,4</sup> have been reported among large numbers of azide compounds found in the Cambridge Structural Database.<sup>1a,5</sup> Therefore, previous investigations of metal–azido systems had mainly focused on low dimensionalities. However, high-dimensional networks of metal–azido derivatives are of particular interest because of their novel topology and enhancement of bulk magnetic properties as well as their magnetostructural correlations.<sup>6</sup>

A common strategy employed for the synthesis of a high-dimensional metal–azido system is the further extension of metal–azido assemblies using additional organic linkers.<sup>7</sup> To date, a large number of complementary organic ligands have

<sup>a</sup> Beijing Key Laboratory for Green Catalysis and Separation, Department of Chemistry and Chemical Engineering, College of Environmental and Energy Engineering, Beijing University of Technology, Beijing 100124, PR China. E-mail: jrli@bjut.edu.cn

<sup>b</sup> Departamento de Química Inorgànica, Universitat de Barcelona, Diagonal 647, Barcelona 08028, Spain

† Electronic supplementary information (ESI) available: Details of structure refinement, PXRD patterns, and FT-IR spectra of reported new compounds. CCDC 1052035–1052036. For ESI and crystallographic data in CIF or other electronic format see DOI: 10.1039/c5ce00531k



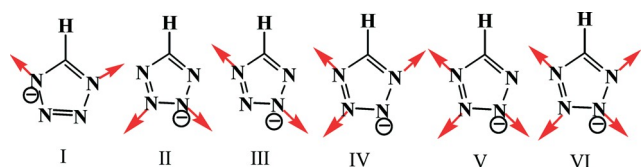
Scheme 1 Different bridging modes of the azide anion.

been employed in this regard.<sup>7</sup> Among them, five-membered heterocyclic azoles (triazoles, tetrazoles, *etc.*) and their derivatives have drawn much attention due to their strong  $\sigma$ -electron donors to metals, diverse coordination modes, and strong super-exchange capacity.<sup>8</sup> As multi-functional bridging ligands, tetrazole derivatives have been widely investigated in recent years in coordination polymer chemistry due to the excellent coordination ability of the four nitrogen atoms in the tetrazole group.<sup>9</sup> Simultaneously, there were also several examples in which tetrazole derivatives act as complementary organic ligands to fabricate high-dimensional magnetic metal–azido networks.<sup>8b,c,9a–e,13a–c,14a,b,15a–f</sup> However, as far as we know, a complex that has both a parent tetrazolate and an azide used together has not been reported until now, although tetrazolate itself has rich coordination modes (Scheme 2) and can be used as a good organic linker for transferring magnetic coupling. On the other hand, the combination of azide and tetrazolate anions in one complex could result in highly N-rich systems, which may be good candidates for high-energy materials. Herein, we report the tuned synthesis (Fig. 1), crystal structure, and magnetic properties of two new tetrazolate–azido-bridged  $\text{Cu}(\text{II})$  coordination polymers:  $[\text{Cu}(\text{tz})(\text{N}_3)]_n$  (1) and  $[\text{Cu}(\text{tz})(\text{N}_3)(\text{NH}_3)_2]_n$  (2). Both 1 and 2 possess distinct 3D network structures being topologically described as a 3-connected *srs* ( $\text{SrSi}_2$ )-type net and a 4-connected *cds* ( $\text{CdSO}_4$ )-type net, respectively, and show antiferrimagnetic properties.

## Experimental section

### Materials and general methods

All general reagents and solvents (AR grade) were commercially available and used as-received. Distilled water was used in hydrothermal synthesis. Elemental analyses were performed on a Perkin-Elmer 240C analyzer. IR spectra were measured on a TENSOR 27 OPUS (Bruker) FT-IR spectrometer with KBr pellets. Powder X-ray diffraction (PXRD) patterns were recorded on a Rigaku D/Max-2500 diffractometer at 40 kV and 100 mA with a Cu-target tube and a graphite monochromator. Simulation of the PXRD patterns was carried out using the single-crystal data and diffraction-crystal module of the *Mercury* program available free of charge *via* the internet at <http://www.iucr.org>. Magnetic data were collected using crushed crystals of the sample on a Quantum Design PPMS-9T magnetometer. Data were corrected using Pascal's constants to calculate the diamagnetic susceptibility. During magnetic measurement, the powder sample was enwrapped



Scheme 2 Different coordination modes of the tetrazolate (tz) anion.

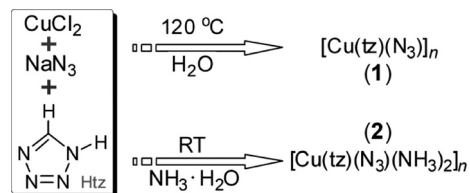


Fig. 1 The synthesis process of 1 and 2.

by a film and then fixed in the tube. The background of the film was corrected.

### Synthesis of complexes

$[\text{Cu}(\text{tz})(\text{N}_3)]_n$  (1). Complex 1 was prepared by a hydrothermal reaction. 10 mL of  $\text{H}_2\text{O}$  solution containing Htz (14 mg, 0.2 mmol),  $\text{CuCl}_2 \cdot 2\text{H}_2\text{O}$  (34 mg, 0.2 mmol), and sodium azide (20 mg, 0.3 mmol) was sealed in a 25 mL Teflon-lined stainless steel container and heated at 120 °C for 3 days. Black crystals were collected, washed with acetone, and then dried in air (yield: 31% based on  $\text{CuCl}_2 \cdot 2\text{H}_2\text{O}$ ). The PXRD pattern and FT-IR spectrum of 1 are shown in Fig. S1 and S2, respectively, in the ESI.† Anal. calcd for  $\text{CHCuN}_7$ : C, 6.88; H, 0.58; N, 56.14. Found: C, 6.81; H, 0.61; N, 56.09.

$[\text{Cu}(\text{tz})(\text{N}_3)(\text{NH}_3)_2]_n$  (2). 10 mL of ammonia solution containing Htz (14 mg, 0.2 mmol),  $\text{CuCl}_2 \cdot 2\text{H}_2\text{O}$  (34 mg, 0.2 mmol), and sodium azide (33 mg, 0.5 mmol) in a glass vial was left at room temperature and solvent evaporation for three days was allowed to occur. Black crystals were collected, washed with acetone, and then dried in air (yield: 28% based on  $\text{CuCl}_2 \cdot 2\text{H}_2\text{O}$ ). The PXRD pattern and FT-IR spectrum of 2 are shown in Fig. S1 and S2, respectively, in the ESI.† Anal. calcd for  $\text{CH}_7\text{CuN}_9$ : C, 5.76; H, 3.38; N, 60.41. Found: C, 5.80; H, 3.43; N, 60.35.

Caution! Azide derivatives are potentially explosive, particularly in this highly N-rich system with metal ions. Although we have not encountered problems in handling the  $\text{Cu}(\text{II})$  systems during this work, only a small amount of them should be prepared and managed with great caution, especially in hydrothermal synthesis.

### Single-crystal X-ray crystallography

Single-crystal X-ray diffraction data were collected on a Rigaku R-AXIS RAPID IP X-ray diffractometer equipped with a fine-focus sealed-tube X-ray source (graphite monochromated  $\text{Mo-K}\alpha$  radiation,  $\lambda = 0.71073$  Å). Suitable single crystals were directly picked up from the mother liquor, attached to a glass loop for data collection at 20 °C. Raw data collection and reduction were carried out using RAPID-AUTO and CrystalStructure software, respectively.<sup>10</sup> Structures were solved by direct methods and refined by full-matrix least-squares on  $F^2$  with anisotropic displacement using the SHELXTL software package.<sup>11</sup> Non-hydrogen atoms were refined with anisotropic displacement parameters during the final cycles. Hydrogen atoms of the ligands were calculated in ideal positions with isotropic displacement parameters.

CCDC 1052035 (1) and 1052036 (2) contain the supplementary crystallographic data for this paper. Crystallographic data and structural refinements, and selected bond distances and angles for 1 and 2 are listed in Tables 1 and 2, respectively.

## Results and discussion

### Synthesis and general characterization

Complexes 1 and 2 were synthesized as single crystals under different reaction conditions: hydrothermal conditions in water and at room temperature in ammonia solution, respectively, through the reaction of  $\text{CuCl}_2$ ,  $\text{NaN}_3$ , and Htz. As discussed below, 1 and 2 have different compositions and structures, demonstrating that the synthesis conditions have a great effect on the outcomes in this tetrazolate–azido system. We also investigated the same reaction by varying the solvents and reaction temperatures. For the water at room temperature, although we tried a lot of times under different conditions through changing the ratios of reactants and the concentration of the reaction system, we did not get a product which can be structurally characterized through single-crystal or powder X-ray diffraction at room temperature. In most cases, blue amorphous powders were obtained, the structures of which are difficult to determine. With  $\text{CH}_3\text{OH}$  or  $\text{CH}_3\text{CN}$  acting as the solvent at room temperature and higher temperatures of 60, 80, and 100 °C, respectively, again blue or green amorphous powders were obtained in each case, not crystalline products. However, with *N,N*-dimethylformamide (DMF), at both room temperature and higher temperatures up to 120 °C, no solid product was formed and a yellow or brown clear solution was always obtained. For all obtained amorphous powders, we did not further analyze their structures in this work. The phase purity of the bulky

products of 1 and 2 has been examined by PXRD. Fig. S1† shows the measured PXRD patterns of 1 and 2 and their simulated ones based on single-crystal structure analyses. It is obvious that the measured patterns match with the simulated ones, being indicative of pure products. The IR spectra (Fig. S2†) of 1 and 2 show very strong absorption bands at 2092 and 2038  $\text{cm}^{-1}$ , respectively, which can be attributed to the asymmetric stretching vibrations of the coordinated azide ions. The absorption bands in the 1000–1500  $\text{cm}^{-1}$  range are characteristic of  $\nu(\text{C-N})$ ,  $\nu(\text{N-N})$ , and  $\delta(\text{N-N-N})$  of the tetrazolate ligand.<sup>12</sup> The two complexes are stable in air at ambient temperature and insoluble in most solvents such as water, alcohol and acetone, indicating their polymeric nature as realized by structural determination. In addition, due to their potentially explosive nature (the N contents are as high as 50% and 60% in 1 and 2, respectively), thermal analyses of 1 and 2 were not carried out in this work.

### Crystal structures

$[\text{Cu}(\text{tz})(\text{N}_3)]_n$  (1). Single-crystal structural determination of complex 1 reveals that it is a 3D coordination polymer and crystallizes in the orthorhombic space group  $P2_12_12_1$ . As shown in Fig. 2b, the crystallographic asymmetric unit of 1 consists of one  $\text{Cu}(\text{II})$  cation, one tz anion, and one azido anion. The  $\text{Cu}(\text{II})$  ion adopts a five-coordinated configuration in a square-pyramidal coordination environment (Fig. 2a and b). The basal plane of the square-pyramid consists of four nitrogen atoms, two from different tetrazole ligands [1.988(2) Å for  $\text{Cu}(\text{II})\text{--N}(\text{I}3\text{D})$  and 1.990(2) Å for  $\text{Cu}(\text{II})\text{--N}(\text{I}4\text{E})$ ] and two from different azide groups [2.001(2) Å for  $\text{Cu}(\text{II})\text{--N}(\text{I}5)$  and 2.006(2) Å for  $\text{Cu}(\text{II})\text{--N}(\text{I}5\text{F})$ ]. The tz and azido groups occupy the opposite positions of the basal plane in the square-pyramidal environment. The apical position is occupied by a nitrogen atom from a tetrazole ligand with an obviously elongated Cu–N bond [2.218(2) Å for  $\text{Cu}(\text{II})\text{--N}(\text{I}1)$ ] (see Table 2). The  $\text{Cu}(\text{II})$  center deviates from the mean equatorial plane by 0.2296(2) Å toward the apical site. In the structure, each azide anion links two  $\text{Cu}(\text{II})$  atoms in single end-on (EO) mode to form a zig-zig azide-bridged  $\text{Cu}(\text{II})$  chain in the crystallographic *a* direction, with Cu–N distances of 2.001(2) Å and 2.006(2) Å, respectively, being in the normal Cu–N range in EO azide-bridged  $\text{Cu}(\text{II})$  chains.<sup>13</sup> In the chain, the Cu–N–Cu angle is 115.98(9)° and the adjacent  $\text{Cu}\cdots\text{Cu}$  separation is 3.3978(6) Å. The  $\text{Cu}\cdots\text{Cu}$  distance is a little bit shorter than that in some single EO azide– $\text{Cu}(\text{II})$  chains,<sup>2,3,13</sup> probably due to bridging of the tz groups. As additional bridges, each tz anion adopts a 3-coordination mode (mode IV in Scheme 2) to bond two adjacent  $\text{Cu}(\text{II})$  ions of the azide– $\text{Cu}(\text{II})$  chain using two tz nitrogen atoms and to bridge another  $\text{Cu}(\text{II})$  atom from a different azide– $\text{Cu}(\text{II})$  chain. All tz groups are parallel to the *a* direction, but the tz groups bridge azide– $\text{Cu}(\text{II})$  chains in two different directions to finally form a 3D framework with small parallelogram channels running along the *a* direction (Fig. 2c). In the 3D framework, both tz and azide groups act as bridging ligands, so the whole 3D

Table 1 Crystal data and structure refinement parameters of 1 and 2

Complex	1	2
Formula	$\text{CuCHN}_7$	$\text{CuCH}_2\text{N}_9$
Formula weight	174.63	208.70
Crystal system	Orthorhombic	Monoclinic
Space group	$P2_12_12_1$	$C2/c$
<i>a</i> , Å	6.7352(13)	11.804(2)
<i>b</i> , Å	7.5089(15)	5.7178(11)
<i>c</i> , Å	9.6823(19)	10.984(2)
$\alpha$ , °	90	90
$\beta$ , °	90	115.84(3)
$\gamma$ , °	90	90
<i>V</i> , Å <sup>3</sup>	489.67(17)	667.2(2)
<i>Z</i>	4	4
<i>D</i> , g cm <sup>−3</sup>	2.369	2.078
$\mu$ , mm <sup>−1</sup>	4.353	3.221
Independent reflections	1117	585
<i>R</i> <sub>int</sub>	0.0349	0.0357
<i>R</i> [ <i>i</i> ]/ $\sigma$ ( <i>i</i> ) > 2]	0.0169	0.0318
<i>R</i> <sub>w</sub> [ <i>i</i> ]/ $\sigma$ ( <i>i</i> ) > 2]	0.0397	0.0893
Goodness-of-fit on <i>F</i> <sup>2</sup>	1.148	1.142
No. of reflections used	1117	585
No. of parameters refined	82	54
$\Delta\rho_{\text{max}}$ [e Å <sup>−3</sup> ]	0.230	0.970
$\Delta\rho_{\text{min}}$ [e Å <sup>−3</sup> ]	−0.464	−0.604

Table 2 Selected bond lengths (Å) and angles (°) of 1 and 2<sup>a</sup>

$[j\text{Cu}(\text{tz})\mu(\text{N}_3)]_n$ (1)			
Cu(1)–N(3) <sup>i</sup>	1.988(2)	Cu(1)–N(4) <sup>ii</sup>	1.990(2)
Cu(1)–N(5)	2.001(2)	Cu(1)–N(5) <sup>iii</sup>	2.006(2)
Cu(1)–N(1)	2.218(2)	N(3)–Cu(1) <sup>iv</sup>	1.988(2)
N(3) <sup>i</sup> –Cu(1)–N(4) <sup>ii</sup>	166.70(7)	N(3) <sup>i</sup> –Cu(1)–N(5)	93.07(7)
N(4) <sup>ii</sup> –Cu(1)–N(5)	86.33(8)	N(3) <sup>i</sup> –Cu(1)–N(5) <sup>iii</sup>	86.00(7)
N(4) <sup>ii</sup> –Cu(1)–N(1)	91.52(8)	N(5)–Cu(1)–N(5) <sup>iii</sup>	166.63(3)
N(3) <sup>i</sup> –Cu(1)–N(1)	93.58(8)	N(4) <sup>ii</sup> –Cu(1)–N(1)	99.70(8)
N(5)–Cu(1)–N(1)	96.12(8)	N(5) <sup>iii</sup> –Cu(1)–N(1)	97.25(8)
N(2)–N(1)–Cu(1)	114.1(1)	N(2)–N(3)–Cu(1) <sup>iv</sup>	125.5(2)
N(4)–N(3)–Cu(1) <sup>iv</sup>	122.9(2)	N(3)–N(4)–Cu(1) <sup>v</sup>	118.4(2)
N(6)–N(5)–Cu(1)	122.0(2)	N(6)–N(5)–Cu(1) <sup>vi</sup>	119.1(2)
Cu(1)–N(5)–Cu(1) <sup>vi</sup>	115.97(8)		
$[j\text{Cu}(\text{tz})\mu(\text{N}_3)\mu(\text{NH}_3)_2]_n$ (2)			
Cu(1)–N(3)	2.011(3)	Cu(1)–N(1)	2.037(3)
Cu(1)–N(5)	2.493(4)		
N(3) <sup>i</sup> –Cu(1)–N(3)	180.000(1)	N(3) <sup>i</sup> –Cu(1)–N(1) <sup>i</sup>	89.26(11)
N(3)–Cu(1)–N(1) <sup>i</sup>	90.74(11)	N(2)–N(1)–Cu(1)	126.6(2)
N(3)–Cu(1)–N(1)	89.26(11)		

<sup>a</sup> Symmetry codes for 1: (i)  $-x + 2, y - 1/2, -z + 7/2$ ; (ii)  $-x + 5/2, -y + 4, z - 1/2$ ; (iii)  $x - 1/2, -y + 7/2, -z + 3$ ; (iv)  $-x + 2, y + 1/2, -z + 7/2$ ; (v)  $-x + 5/2, -y + 4, z + 1/2$ ; (vi)  $x + 1/2, -y + 7/2, -z + 3$ . Symmetry code for 2: (i)  $-x + 3/2, -y + 3/2, -z + 2$ .

structure can be thought to be constructed through the  $\text{Cu}(\text{II})$  centers coordinated simultaneously by  $\mu$ -1,2,4 bridging tz ligands and  $\mu$ -1,1 (EO) bridging azide anions (Fig. 2a). The bridging modes of azide and tetrazole ligands are significantly responsible for the magnetic properties of the complex as discussed in detail later.

Topologically, each tz ligand connects three adjacent  $\text{Cu}(\text{II})$  ions through three Cu–N bonds, and simultaneously each  $\text{Cu}(\text{II})$  ion links with three tz ligands. Thus, each tz ligand

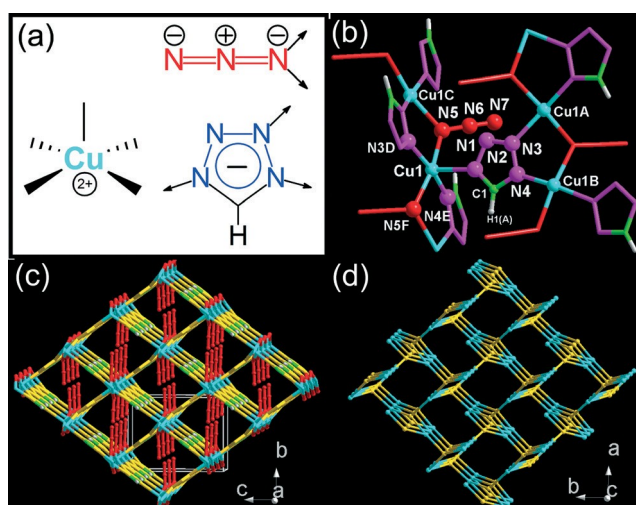


Fig. 2 (a) Scheme showing the linkage modes of tz,  $\text{Cu}(\text{II})$ , and azide in 1. (b) ORTEP view of the main unit of 1 with atom numbering scheme. (c) 3D network structure of 1 viewed along the crystallographic *a* axis;  $\text{Cu}(\text{II})$  is shown as cyan, N of tz as gold, C as green, H as white, and azide as red. (d) Schematic representation of the topological net of 1 with tz being represented by 3-connected yellow spheres and  $\text{Cu}(\text{II})$  by cyan.

and  $\text{Cu}(\text{II})$  ion can be defined as a three-connected node. As the azide group only acts as an additional bridge, it is not necessary to consider it in the topological analysis. Based on this analysis, the structure of 1 can be described as a 3-connected *srs* ( $\text{SrSi}_2$ )-type net with a point symbol of  $\{10^3\}$  (Fig. 2d).

$[j\text{Cu}(\text{tz})\mu(\text{N}_3)\mu(\text{NH}_3)_2]_n$  (2). Single-crystal structural determination reveals that 2 also has a 3D framework structure, but different from that of 1 and crystallizes in the monoclinic space group  $C2/c$ . As shown in Fig. 3b, the crystallographic asymmetric unit of 2 consists of half a  $\text{Cu}(\text{II})$  center, half a tz ligand, half an azido anion, and one ammonia molecule. The

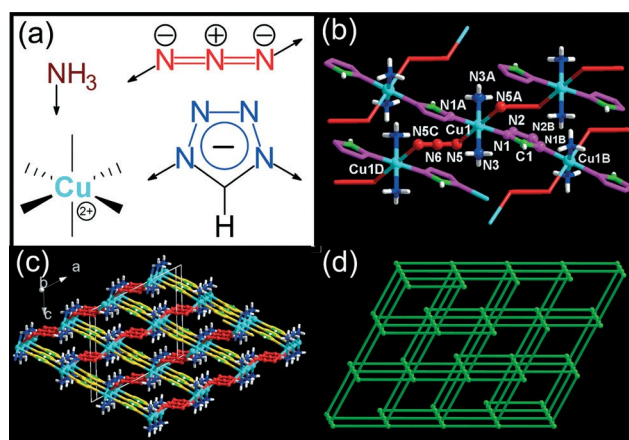


Fig. 3 (a) Scheme showing the linkage modes of tz,  $\text{Cu}(\text{II})$ , and azide in 2. (b) ORTEP view of the main unit of 2 with atom numbering scheme. (c) 3D network structure of 2 viewed along the crystallographic *b* axis;  $\text{Cu}(\text{II})$  is shown as cyan, N of tz as gold, C as green, H as white, and azide as red. (d) Schematic representation of the topological net of 2 with  $\text{Cu}(\text{II})$  being represented by 4-connected green spheres.



$\text{Cu}(\text{II})$  center locates at an inverse center and takes a distorted octahedral coordination configuration sustained by six nitrogen atoms (Fig. 3a and b). The four nitrogen atoms at the equatorial plane are from two tz ligands and two ammonia molecules with the Cu–N bond lengths being 2.037(3) Å and 2.011(3) Å, respectively. Two nitrogen atoms of distinct azide ions are located symmetrically at the two axial positions, with a Cu–N bond length of 2.493(4) Å (see Table 2). Due to the strong Jahn–Teller effect of the  $\text{Cu}(\text{II})$  ion, the Cu–N bond lengths in the axial positions are remarkably elongated, which would be significantly responsible for the magnetic properties as discussed later. As a whole, in 2, each tz ligand adopts a 2-coordination mode (mode I in Scheme 2) to link two  $\text{Cu}(\text{II})$  centers to form a tz-bridged  $\text{Cu}(\text{II})$  chain, in which the intra-chain  $\text{Cu}\cdots\text{Cu}$  distance is 6.061(3) Å. Each azide anion adopts a *trans*- $\mu$ -1,3 (EE) mode to bond two  $\text{Cu}(\text{II})$  centers in two adjacent tz-bridged chains (giving an inter-chain  $\text{Cu}\cdots\text{Cu}$  distance of 6.5580(9) Å), and each  $\text{Cu}(\text{II})$  is thus linked by two tz and two azide groups. Interestingly, the azide groups bridge tz- $\text{Cu}(\text{II})$  chains in two different directions to finally form a 3D framework with tetragonal channels along the *b* axis (Fig. 3c). It should be pointed out that the  $\mu$ -1,3 (EE) azido linker always links the metal centers in the most favorable *trans* fashion with a few exceptions showing a *cis*-type coordination.<sup>14</sup>

From the viewpoint of structural topology, both azido and tz ligands act as linear bridges, thus the present framework of 2 can be described as a *cds* ( $\text{CdSO}_4$ )-type net with a point symbol of  $\{6^5\cdot 6^8\}$ , based on the 4-connected  $\text{Cu}(\text{II})$  centers (Fig. 3d).

### Magnetic properties

Variable temperature susceptibility data for complex 1 were collected with an applied field of 0.2 T in the 300 to 2 K temperature range.  $\chi_M$  vs. *T* and  $\chi_M T$  vs. *T* plots can be found in Fig. 4a. The  $\chi_M T$  value at room temperature is 0.33, slightly below the expected value for one  $\text{Cu}(\text{II})$  ion with  $g = 2.0$  ( $S = 1/2$ ,  $g = 2.0$ ,  $\chi_M T = 0.375 \text{ cm}^3 \text{ K mol}^{-1}$ ). As the temperature decreases, so does the  $\chi_M T$  product, indicating antiferromagnetic interaction within the 3D network of 1. The magnetization was measured at 2 K in the 0 to 5 T applied field range. As can be seen in Fig. 4b, it rises without reaching saturation. At 5 T, the reduced magnetization value is 0.06, which supports the strong antiferromagnetic interactions dominant in 1, leading to a diamagnetic ground state. The magnetic structure of 1 is formed by infinite chains of 5-coordinated  $\text{Cu}(\text{II})$  ions with a square-pyramidal geometry bridged by EO azido ligands and tetrazolate ligands. Generally, the EO mode azido ligand can mediate both ferro- and antiferromagnetic interactions depending on the Cu–N–Cu bond angle. For the  $\text{Cu}(\text{II})$  system, it is observed that when this angle is less than  $108^\circ$ , the complex shows ferromagnetic properties, and when it is larger than  $108^\circ$ , the magnetic interaction between the paramagnetic centers is antiferromagnetic in nature.<sup>15</sup> In 1, the Cu–N( $\text{N}_3$ )–Cu angle is  $115.98(9)^\circ$ , thus the coupling through

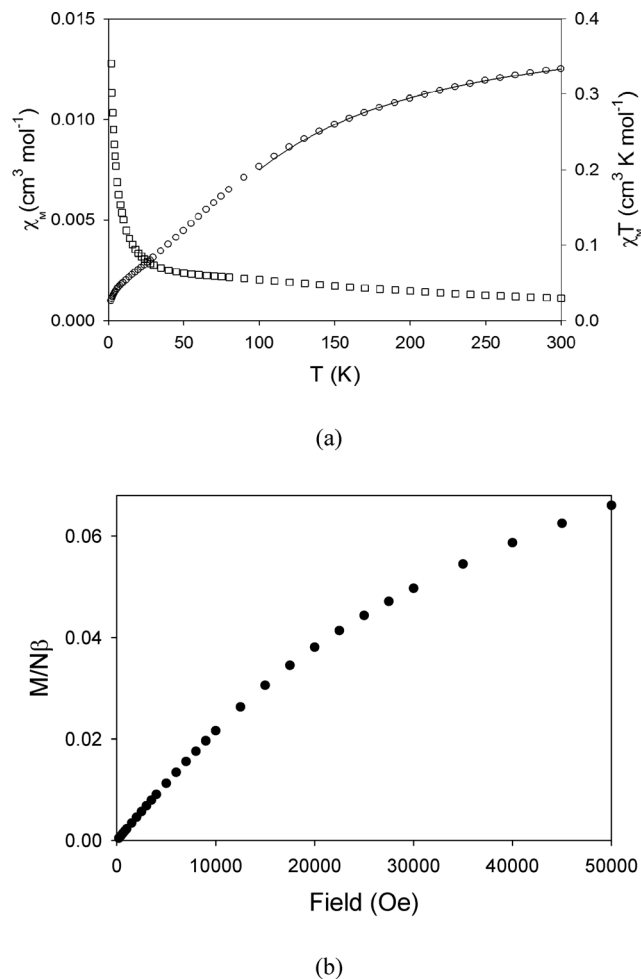


Fig. 4 (a) Temperature dependence of the magnetic susceptibility of 1 at an applied DC field of 0.2 T ( $\chi_M T$ , empty circles;  $\chi_M$ , empty squares; the solid line is the best fit to the experimental data). (b) Field dependence of the magnetization of 1 at 2 K.

the azido ligand should be antiferromagnetic.<sup>16</sup> The chains are linked into a square grid by tetrazolate ligands that mediate the interaction between the magnetic orbital  $|\text{d}_{x^2-y^2}\rangle$  of the  $\text{Cu}(\text{II})$  ions in one chain and a full  $\text{d}_{z^2}$  orbital of the  $\text{Cu}(\text{II})$  ions in the neighbouring chain.<sup>17</sup> This type of interaction is known to lead to weak ferromagnetic exchange. The magnetic susceptibility follows the Curie–Weiss law at temperatures above 100 K. Given the fact that the antiferromagnetic interaction along the chains will dominate the magnetic behaviour of 1, high-temperature data were modelled by assuming isolated infinite chains. An equation for an infinite chain of  $\text{Cu}(\text{II})$  ions<sup>18</sup> with  $S = 1/2$  was used to fit the experimental susceptibility data above 100 K; the best fit is shown in Fig. 4a as a solid line and the fitting parameters were  $g = 2.2$  and  $J = -41.0 \text{ cm}^{-1}$ .

Fig. 5a shows the temperature dependence of the magnetic susceptibility of complex 2 at an applied DC field of 1.0 T in the 2–300 K range and at 500 G below 25 K. As can be seen in the plot of  $\chi_M T$  per  $\text{Cu}(\text{II})$  ion vs. *T*, there is no field dependence of the magnetic behaviour of 2. As the

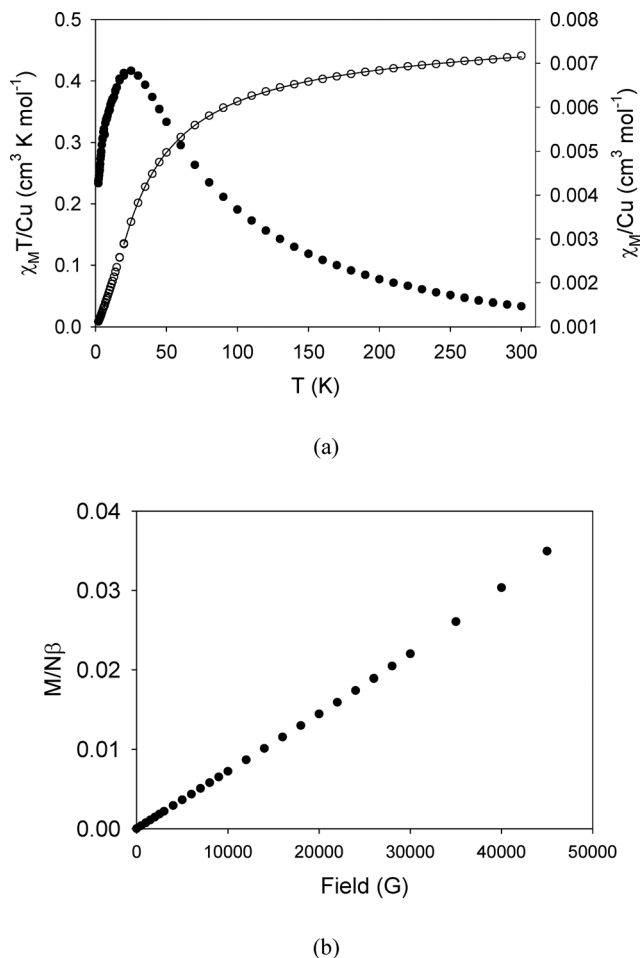


Fig. 5 (a) Temperature dependence of the magnetic susceptibility of **2** at an applied DC field of 1.0 T ( $\chi_M T$ , empty circles;  $\chi_M$ , full circles; the solid line is the best fit to the experimental data). (b) Field dependence of the magnetization of **1** at 2 K.

temperature decreases, the susceptibility per  $\text{Cu(II)}$  ion,  $\chi_M$ , rises to a maximum at 23 K and then drops to a value of  $0.04 \text{ cm}^3 \text{ mol}^{-1}$  at 2 K. The  $\chi_M T$  product per  $\text{Cu(II)}$  ion has a value of  $0.441 \text{ cm}^3 \text{ K mol}^{-1}$  at 300 K, which agrees well with that for an isolated  $\text{Cu(II)}$  ion. As the temperature decreases, so does the  $\chi_M T$  product, down to a value of  $0.008 \text{ cm}^3 \text{ K mol}^{-1}$  at 2 K. The magnetization increases linearly to a value of 0.04 with field as this increases from 0 to 50 000 G, never reaching saturation, as seen in Fig. 5b. All these clearly indicate antiferromagnetic interactions between the  $\text{Cu(II)}$  ions in **2**. The crystal structure shows a 3D arrangement of chains of  $\text{Cu(II)}$  ions linked by EE azide ligands; along the chains, each pair of  $\text{Cu(II)}$  atoms is bridged by tetrazole. EE azide bridging is known to lead to strong antiferromagnetic coupling but this is not the case in **2**, due to its particular structure. In **2**, each  $\text{Cu(II)}$  is 6-coordinated in a distorted octahedral fashion; the distortion takes the form of a very pronounced axial elongation along the  $d_{z^2}$  orbital, perpendicular to the  $\text{Cu(II)}$  magnetic orbital,  $d_{x^2-y^2}$ . The  $\text{Cu-N(N}_3\text{)}$  bonds are always in this elongated axis (the  $\text{Cu-N}$  distance is  $2.493(4) \text{ \AA}$ ), thus, the interaction through this azide bridge is

expected to be very weak or negligible. Along the chains, antiferromagnetic interaction can be predicted to be mediated by tetrazole bridges, similar to that found in  $\text{Cu(II)}$  complexes with bridging imidazolate ligands,<sup>19</sup> in which the bridging mode of imidazolate is similar to that of tetrazolate in **2**. Taking all these into account, the system was treated as an isolated chain. The magnetic data above 20 K were fitted to a simple 1D chain model<sup>18</sup> (the Hamiltonian is written as  $\hat{H} = -2JS_1S_2$ ) and the inter-chain interactions were included in the model as a Curie–Weiss constant. A good agreement was obtained using the linear chain model of  $S = 1/2$ , and the best fit, shown in Fig. 5a as a solid line, was obtained for  $J = -8.62 \text{ cm}^{-1}$ ,  $g = 2.22$ ,  $\text{TIP} = 37 \times 10^{-6} \text{ cm}^3 \text{ mol}^{-1}$  and a Curie–Weiss constant of  $-12 \text{ K}$ .

## Conclusion

In this work, through tuning the reaction conditions, we have synthesized two novel tetrazolate–azido bridged  $\text{Cu(II)}$  coordination polymers with different 3D network structures. To the best of our knowledge, this is the first example of using a parent tetrazole and an azide together in preparing magnetic complexes. **1** features  $\mu$ -1,1 (EO) azide and  $\mu$ -1,2,4 tetrazolate coordination modes to link  $\text{Cu(II)}$  atoms to form a 3-connected *srs* ( $\text{SrSi}_2$ )-type net, while **2** features  $\mu$ -1,3 (EE) azide and  $\mu$ -1,4 tetrazolate linkage modes to give a 4-connected *cds* ( $\text{CdSO}_4$ )-type net. These two complexes show antiferrimagnetic properties, being well-correlated with their structures. This work extends the research of engineering azide–metal magnetic coordination polymer systems.

## Acknowledgements

This work was financially supported by the NSFC (no. 21271015, 21322601, and U1407119), the Program for New Century Excellent Talents in University (no. NCET-13-0647) and the Beijing Municipal Natural Science Foundation (no. 2132013). ECS acknowledges financial support from the Spanish Government (grant CTQ2012-32247).

## References

- (a) J. Ribas, A. Escuer, M. Monfort, R. Vicente, R. Cortes, L. Lezama and T. Rojo, *Coord. Chem. Rev.*, 1999, 193–195, 1027; (b) J. S. Miller and M. Drillon, *Magnetism: Molecules to Materials. Models and Experiments; vol. 1 and Molecule-based Magnets; vol. 2*, Wiley-VCH, 2001; (c) D. Maspoch, D. Ruiz-Molina and J. Veciana, *Chem. Soc. Rev.*, 2007, 36, 770; (d) R. Sessoli and A. K. Powell, *Coord. Chem. Rev.*, 2009, 253, 2328; (e) M. Zhu, Y.-G. Li, Y. Ma, L.-C. Li and D.-Z. Liao, *Inorg. Chem.*, 2013, 52, 12326; (f) J. N. Boynton, J.-D. Guo, J. C. Fettinger, C. E. Melton, S. Nagase and P. P. Power, *J. Am. Chem. Soc.*, 2013, 135, 10720; (g) J.-P. Zhao, Q. Yang, Z.-Y. Liu, R. Zhao, B.-W. Hu, M. Du, Z. Chang and X.-H. Bu, *Chem. Commun.*, 2012, 48, 6568.
- (a) Y.-Z. Zhang, H.-Y. Wei, F. Pan, Z.-M. Wang, Z.-D. Chen and S. Gao, *Angew. Chem., Int. Ed.*, 2005, 44, 5841; (b) Y.-F.

- Zeng, X. Hu, F.-C. Liu and X.-H. Bu, *Chem. Soc. Rev.*, 2009, 38, 469; (c) S. Mukherjee, Y. P. Patil and P. S. Mukherjee, *Dalton Trans.*, 2012, 41, 54; (d) Y.-Y. Zhu, C. Cui, N. Li, B.-W. Wang, Wang Z.-M. and S. Gao, *Eur. J. Inorg. Chem.*, 2013, 3101.
- 3 (a) K. C. Mondal and P. S. Mukherjee, *Inorg. Chem.*, 2008, 47, 4215; (b) P. S. Mukherjee, T. K. Maji, G. Mostafa, T. Mallah and N. R. Chaudhuri, *Inorg. Chem.*, 2000, 39, 5147.
- 4 (a) M. A. S. Goher, J. Cano, Y. Journaux, M. A. M. Abu-Youssef, F. A. Mautner, A. Escuer and R. Vicente, *Chem. – Eur. J.*, 2000, 6, 778; (b) O. Sengupta, R. Chakrabarty and P. S. Mukherjee, *Dalton Trans.*, 2007, 4514.
- 5 (a) M. A. M. Abu-Youssef, A. Escuer, M. A. S. Goher, F. A. Mautner, G. J. Reib and R. Vicente, *Angew. Chem., Int. Ed.*, 2000, 39, 1624; (b) X.-T. Liu, X.-Y. Wang, W.-X. Zhang, P. Cui and S. Gao, *Adv. Mater.*, 2006, 18, 2852; (c) T.-F. Liu, D. Fu, S. Gao, Y.-Z. Zhang, H.-L. Sun, G. Su and Y.-J. Liu, *J. Am. Chem. Soc.*, 2003, 125, 13976; (d) H. H. Ko, J. H. Lim, H. C. Kim and C. S. Hong, *Inorg. Chem.*, 2006, 45, 8847; (e) A. Escuer, M. A. S. Goher, F. A. Mautner and R. Vicente, *Inorg. Chem.*, 2000, 39, 2107; (f) A. Das, G. M. Rosair, M. S. El Fallah, J. Ribas and S. Mitra, *Inorg. Chem.*, 2006, 45, 3301; (g) Z. Shen, J.-L. Zuo, S. Gao, Y. Song, C.-M. Che, H.-K. Fu and X.-Z. You, *Angew. Chem., Int. Ed.*, 2000, 39, 3633; (h) M. Monfort, I. Resino, J. Ribas and H. Stoeckli-Evans, *Angew. Chem., Int. Ed.*, 2000, 39, 191; (i) Y. S. You, J. H. Yoon, H. C. Kim and C. S. Hong, *Chem. Commun.*, 2005, 4116; (j) Z. He, Z.-M. Wang, S. Gao and C.-H. Yan, *Inorg. Chem.*, 2006, 45, 6694; (k) E.-Q. Gao, Y.-F. Yue, S.-Q. Bai, Z. He and C.-H. Yan, *J. Am. Chem. Soc.*, 2004, 126, 1419.
- 6 (a) F.-C. Liu, Y.-F. Zeng, J.-R. Li, X.-H. Bu, H.-J. Zhang and J. Ribas, *Inorg. Chem.*, 2005, 44, 7298; (b) F.-C. Liu, Y.-F. Zeng, J. Jiao, J.-R. Li, X.-H. Bu, J. Ribas and S. R. Batten, *Inorg. Chem.*, 2006, 45, 6129; (c) F.-C. Liu, Y.-F. Zeng, J. Jiao, X.-H. Bu, J. Ribas and S. R. Batten, *Inorg. Chem.*, 2006, 45, 2776; (d) X.-M. Zhang, Y.-F. Zhao, W.-X. Zhang and X.-M. Chen, *Adv. Mater.*, 2007, 19, 2843.
- 7 (a) M. A. M. Abu-Youssef, A. Escuer, F. A. Mautner and L. Öhrström, *Dalton Trans.*, 2008, 3553; (b) A. Escuer and G. Aromí, *Eur. J. Inorg. Chem.*, 2006, 4721; (c) M. S. El Fallah, R. Vicente, J. Tercero, C. Elpelt, E. Rentschler, X. Solans and M. Font-Bardia, *Inorg. Chem.*, 2008, 47, 6322; (d) L. Cheng, W.-X. Zhang, B.-H. Ye, J.-B. Lin and X.-M. Chen, *Eur. J. Inorg. Chem.*, 2007, 2668; (e) X.-Y. Wang, B.-L. Li, X. Zhu and S. Gao, *Eur. J. Inorg. Chem.*, 2005, 3277; (f) S. Martín, M. G. Barandika, L. Lezama, J. L. Pizarro, Z. E. Serna, J. I. R. de Larramendi, M. I. Arriortua, T. Rojo and R. Cortés, *Inorg. Chem.*, 2001, 40, 4109.
- 8 (a) J.-R. Li, Q. Yu, E. C. Sañudo, Y. Tao and X.-H. Bu, *Chem. Commun.*, 2007, 2602; (b) O. Sengupta and P. S. Mukherjee, *Inorg. Chem.*, 2010, 49, 8583; (c) R.-Y. Li, X.-Y. Wang, T. Liu, H.-B. Xu, F. Zhao, Z.-M. Wang and S. Gao, *Inorg. Chem.*, 2008, 47, 8134.
- 9 (a) A. Rodríguez, R. Kivekäs and E. Colacio, *Chem. Commun.*, 2005, 5228; (b) M. Dincă, A. F. Yu and J. R. Long, *J. Am. Chem. Soc.*, 2006, 128, 8904; (c) M. Dincă and J. R. Long, *J. Am. Chem. Soc.*, 2007, 129, 11172; (d) X. Xue, X.-S. Wang, L.-Z. Wang, R.-G. Xiong, B. F. Abrahams, X.-Z. You, Z.-L. Xue and C. M. Che, *Inorg. Chem.*, 2002, 41, 6544; (e) J. Tao, Z.-J. Ma, R.-B. Huang and L.-S. Zheng, *Inorg. Chem.*, 2004, 43, 6133.
- 10 *Rigaku, RAPID-AUTO*, Rigaku Corporation, Tokyo, Japan, 2004; *Rigaku/MS-CrystalStructure*, Rigaku/MS-C Inc, The Woodlands, Texas, USA, 2004.
- 11 G. M. Sheldrick, *Acta Crystallogr., Sect. A: Found. Crystallogr.*, 2008, 64, 112.
- 12 S. C. S. Bugalho, E. M. S. Macoas, M. L. S. Cristiano and R. Fausto, *Phys. Chem. Chem. Phys.*, 2001, 3, 3541.
- 13 (a) A. Biswas, M. G. B. Drew, C. J. Gómez-García and A. Ghosh, *Inorg. Chem.*, 2010, 49, 8155; (b) S. Koner, S. Saha, T. Mallah and K. Okamoto, *Inorg. Chem.*, 2004, 43, 840; (c) M.-H. Zeng, Y.-L. Zhou, W.-X. Zhang, M. Du and H.-L. Sun, *Cryst. Growth Des.*, 2010, 10, 20.
- 14 (a) C. S. Hong, J. Koo, S. K. Son, Y. S. Lee, Y. S. Kim and Y. Do, *Chem. – Eur. J.*, 2001, 7, 4243; (b) Y.-F. Zeng, J.-P. Zhao, B.-W. Hu, X. Hu, F.-C. Liu, J. Ribas, J. Ribas-Ariño and X. H. Bu, *Chem. – Eur. J.*, 2007, 13, 9924.
- 15 (a) X. He, C.-Z. Lu, C.-D. Wu and L.-J. Chen, *Eur. J. Inorg. Chem.*, 2006, 2491; (b) S. S. Tandon, L. K. Thompson, M. E. Manuel and J. N. Bridson, *Inorg. Chem.*, 1994, 33, 5555; (c) J. Ribas, M. Monfort, B. K. Ghosh, X. Solans and M. Font-Bardia, *J. Chem. Soc., Chem. Commun.*, 1995, 2375; (d) J. Ribas, M. Monfort, B. K. Ghosh and X. Solans, *Angew. Chem., Int. Ed. Engl.*, 1994, 33, 2177; (e) G. Viau, G. M. Lambardi, G. De Munno, M. Julve, F. Lloret, J. Faus, A. Caneschi and J. M. Clemente-Juan, *Chem. Commun.*, 1997, 1195; (f) M. A. Aebbersold, M. Gillon, O. Plantevin, L. Pardi, O. Kahn, I. Bergerat, V. Seggern, L. Ohrstrom, A. Grand and E. Lelievre-Berna, *J. Am. Chem. Soc.*, 1998, 120, 5238.
- 16 E. Ruiz, J. Cano, S. Alvarez and P. Alemany, *J. Am. Chem. Soc.*, 1998, 120, 11122.
- 17 O. Kahn, *Molecular Magnetism*, VCH, New York, 1993.
- 18 W. E. Estes, D. P. Gavel, W. E. Hatfield and D. J. Hodgson, *Inorg. Chem.*, 1978, 17, 1417.
- 19 P. Chaudhuri, I. Karpenstein, M. Winter, M. Lengen, C. Butzlaff, E. Bill, A. X. Trautwein, U. Flörke and H. J. Haupt, *Inorg. Chem.*, 1993, 32, 888.